Confinement-enhanced biexciton binding energy in semiconductor quantum dots

K. I. Kang,* A. D. Kepner,* S. V. Gaponenko,† S. W. Koch,* Y. Z. Hu, and N. Peyghambarian
Optical Sciences Center, University of Arizona, Tucson, Arizona 85721
(Received 19 July 1993)

Experimental observation of the ground-state biexciton transition in CdS_xSe_{1-x} quantum dots in glass is presented in a three-beam experiment, involving a probe, a pump, and a saturating laser pulse. The observed quantum-dot biexciton ground state has a strongly enhanced binding energy compared to the bulk as theoretically predicted. The biexciton binding energy is measured as a function of quantum-dot size and the results are compared with calculations.

Since the first observation of carrier confinement in semiconductor microcrystallites in a glass matrix, quasi-zero-dimensional systems, also called quantum dots, have been extensively investigated both theoretically and experimentally.[1,2] The first simple theoretical model of Efros and Efros[1] and Brus,[3] a one-electron-hole pair (exciton) model using an effective-mass approximation based on a simple parabolic band, has been modified substantially. The modifications have included the electron-hole Coulombic interaction,[4] the dielectric polarization,[3] and the confinement-induced band mixing.[5] The predicted confinement-induced mixing of the valence bands in quantum dots has been confirmed through two-photon absorption experiments in CdS.[5] The advanced model also predicts the existence of the biexciton ground state, which is a bound state of two electron-hole pairs within a single dot.[4]

Prior differential transmission measurements in II-VI semiconductor quantum dots have revealed bleaching of the lowest quantum confined transition (hereafter referred to as the lowest exciton) and induced absorption above it. Bleaching at the exciton resonance is explained by phase-space filling of the ground state of the exciton; the induced absorption above the exciton is attributed to transitions to excited states of the biexciton which are not stable in bulk. Our theory predicts a biexciton ground state with a positive binding energy, suggesting the presence of an induced absorption feature *below* the exciton resonance. The lack of observed induced absorption below the exciton resonance in prior experiments in quantum dots has been attributed to the broad bleaching signal of the exciton.[4] For small homogeneous broadening the biexciton binding energy can be estimated using the energy separation between the exciton and the lower energy-induced absorption peak. (This may be seen from the biexciton energy as given by $E_{xx}=2E_x-E_{bxx}$ with E_x and E_{bxx} being the exciton energy and the biexciton binding energy and noting that $E_{xx}=\hbar\omega+E_x$, leading to $\hbar\omega=E_x-E_{bxx}$ where $\hbar\omega$ is the energy of the absorbed photon—see the inset of Fig. 1.) The theory also predicts an enhanced biexciton binding energy for smaller dot sizes.

In this paper, we present experimental observation of the ground state of the biexciton from an investigation of CdS_xSe_{1-x} quantum dots at 15 K by pump-and-probe spectroscopy with an additional "saturating" laser beam below the pump spectral energy. With this experimental technique, the inhomogeneous contribution of the bleaching signal is effectively controlled by the saturating beam allowing us to observe the transition to the biexciton ground state from the exciton ground state. Inhomogeneous broadening in the quantum dots arises from distributions of size, shape, and stoichiometry of the semiconductor crystallites. Variations in size and shape lead to the different energy levels, and variations in stoichiometry of the CdS_xSe_{1-x} quantum dots lead to different band gaps and band curvatures.

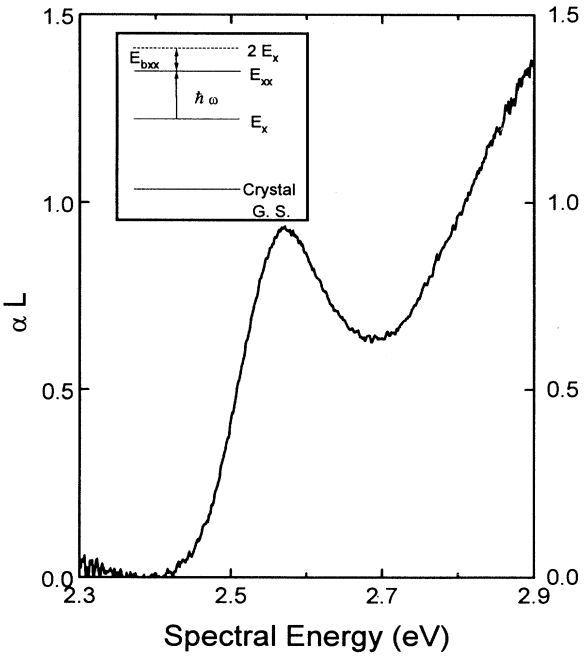

FIG. 1. Linear absorption spectra of CdS_xSe_{1-x} quantum dots at 15 K. This sample was annealed for 24 h at 590 °C and contains quantum dots whose average radius is 23 Å. The resonance at 2.57 eV is the energy of the transition from the crystal ground state to the exciton ground state, E_x. The inset shows energy levels of a quantum dot in a simple single valence-band model.

The samples were prepared using an initial powder of commercial glass containing 0.3 wt. % of CdS, 0.15 wt. % of CdSe, and 0.05 wt. % of S. They were annealed at a relatively low temperature for a relatively long time to enhance normal precipitation growth over the dominant coalescent growth. The sizes of the quantum dots were measured by a small-angle x-ray-scattering technique. We used three samples in which the average radii of the quantum dots are 36, 27, and 23 Å, and which were annealed at 600 °C for 24 h, 590 °C for 36 h, and 590 °C for 24 h, respectively. The total volume fraction of the quantum dot is approximately 0.1%. This is less than the initial volume fraction of Cd, S, and Se because the rest remains in the form of ions in the glass matrix. The sample exhibits broad spectral hole burning when fresh; narrow spectral hole burning occurs after high-intensity laser irradiation.[6] Because of the two different types of spectral hole possible in this sample we present the experimental observation of the ground state of the biexciton in both broad and narrow spectral hole burning situations.

The experimental arrangement is a three-beam setup with a broadband probe covering the whole spectral region of interest, a narrow-band pump tuned inside the first quantum confined transition, and a third saturating beam whose spectral energy is below the pump. The saturator beam is a spectrally narrow source used to constantly saturate the lowest exciton transition of certain sized quantum dots such that these transitions do not participate in the nonlinear spectra. The temporal widths of the pump and the saturating laser beams are about 3 ns, and that for the probe is 5 ns. The saturator arrives at the sample about 1 ns ahead of the pump, and the pump arrives about 1 ns ahead of the probe. To ensure that only excited portions of the sample are probed, we use an $\simeq 100$ μm probe spot and $\simeq 250$ μm saturator and pump spots. The directions of propagation for the pump and probe are almost collinear with about 8° angular separation and the saturator counter propagates with an angular separation with respect to probe being $\simeq 172°$ and with respect to the pump being $\simeq 164°$. For the broad spectral hole burning experiment, we chose "fresh spots" on the sample which had not been previously exposed to high-intensity radiation. For narrow spectral hole burning, we prepared the sample by irradiating with 36 000 pulses of about 5-ns duration from the third harmonic of the Nd:YAG laser (where YAG denotes yttrium aluminum garnet). The average pulse intensity was about 30 MW/cm^2.

The linear absorption spectrum of one of the samples (average quantum-dot radius 23 Å) at 15 K is shown in Fig. 1. The resonance at about 2.57 eV is due to the lowest quantum confined transition, the exciton ground state. Differential transmission spectra ($-\Delta\alpha L$) of the same sample at 15 K are shown in Figs. 2(a) and 2(b). Figure 2(a) is associated with narrow spectral hole burning in the part of sample which had been previously exposed to the high-intensity third harmonic while Fig. 2(b) is associated with the broad spectral hole burning in the fresh part of the sample. The topmost curves have been obtained without the saturator beam, and the rest are with the saturator tuned to different wavelengths, the arrows in the graphs indicating the spectral position of the saturator. In both Figs. 2(a) and 2(b) the pump beam energy and its spectral position remained fixed during the experiment. Without the saturator, we observe only a small shift in the peak of the broad bleaching signal when the pump wavelength is tuned, however in the narrow hole burning situation the peak always lies at the pump spectral energy. As may be seen from the top curves in Figs. 2(a) and 2(b), without the saturator beam the photoexposed sample exhibits an induced absorption on the high-energy side of the bleaching while the fresh sample exhibits a valley. Large broadening of the bleaching in the fresh sample hides the induced absorption there. The bleaching is due to phase-space filling of the ground exciton state, and the induced absorption or valley on the high-energy side is due to excited states of the biexciton. With the saturator beam present, both Figs. 2(a) and 2(b) exhibit clear induced absorptions *below* the spectral energy of the bleaching. This bleaching is not a coherent artifact since the width of the induced absorption is broad

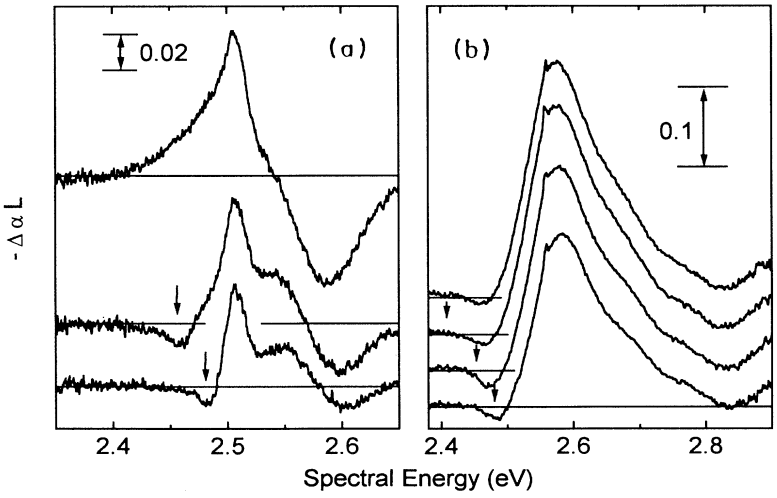

FIG. 2. Differential transmission spectra of CdS_xSe_{1-x} quantum dots at 15 K. (a) is associated with narrow spectral hole burning in the photoexposed sample pumped at 2.50 eV, and (b) is associated with broad spectral hole burning in the fresh sample pumped at 2.53 eV. The intensity of the pump is 340 kW/cm^2, and that of the saturator is 1.36 MW/cm^2. The arrows on the graphs indicate the spectral positions of the saturator.

compared to the spectral width of the saturator and the pump, and there is no coherent coupling artifact at the pump spectral energy. It is expected that any coherent artifact would be much larger at the pump spectral energy since the time separation between the pump and probe is shorter than that between the saturator and the probe. Therefore we attribute this induced absorption to the transition from the ground state of the exciton to the ground state of the biexciton. We also note the shift of the spectral position of the maximum induced absorptions on both sides of the bleaching as the saturator is tuned. This is because for increasing saturator spectral energy the average size of the dots which participate in the nonlinear spectra decreases.

The important role of the saturator in pump-and-probe spectroscopy of an inhomogeneously broadened system can be seen with the following simple scheme: We assume that variation in dot sizes is the only source of inhomogeneous broadening and the saturator beam tuned to the low-energy side of the absorption peak bleaches the lowest exciton transitions of all the quantum dots with larger sizes while it has little influence on the smaller dots. We model the effects of the saturator beam as changing the distribution of sizes of the dots according to the saturator frequency and intensity. The distribution function is assumed to be a step Gaussian, i.e., $f(r) \propto \exp(-(r-R)^2/a^2)$ if $r<(R+\delta)$ and $f(r)=0$ if $r>(R+\delta)$. The parameter δ is used to simulate the bleaching effect of the saturator. With this distribution function and the previously used method of matrix diagonalization,[7] we calculated the differential transmission spectra. In Fig. 3, the computed differential transmission spectra are plotted for quantum dots with $R=0.75a_B$ (where a_B is the exciton Bohr radius) and $a=0.1R$. The homogenous decay constant should be $\gamma=1E_R$ (where E_R is the exciton Rydberg energy) is used. The pump is tuned to the lowest exciton transition energy of the quantum dot of size R. The chosen parameter for δ is (a) ∞, (b) $0.2R$, and (c) 0. Curve (a) shows the differential transmission spectra in the absence of the saturator beam; the ground-state biexciton transition is partially hidden due to inhomogeneous broadening. Curve (b) corresponds to the situation when the detuning of the saturator beam is large. The induced absorption due to the ground-state biexciton is easily observable because of the saturation of the lowest exciton transitions in the larger dots. In curve (c), the saturator beam is tuned closer to the center of the linear absorption peak compared with curve (b). The biexciton induced absorption is more pronounced in this case. In this figure, note that the induced absorption on either side of the bleaching shifts to the blue as the larger-sized quantum dots are removed in correspondence with the experimental data of Fig. 2(a).

The binding energy of the biexciton is estimated by first finding the spectral position of the maximum induced absorption while tuning the saturator below the pump spectral energy. The maximum induced absorption may not be at the saturator spectral energy. The binding energy of the biexciton is estimated from the energy difference between the biexciton and the exciton transition energies as described before. The results of our measured biexciton binding energy are shown in Fig. 4 for various average sizes of the quantum dots.

Note that the biexciton binding energy determined in this way is not accurate since there has been a systematic overestimation. This overestimation is clearly observable in the theoretical calculation of Fig. 3. Measuring the peak-to-valley distance in Fig. 3(c) we obtain approximately $1.4E_R$. The calculated biexciton binding energy is $0.9E_R$. Hence, we see that the combination of homogeneous and inhomogeneous broadening leads to an experimentally unavoidable overestimation of the biexciton

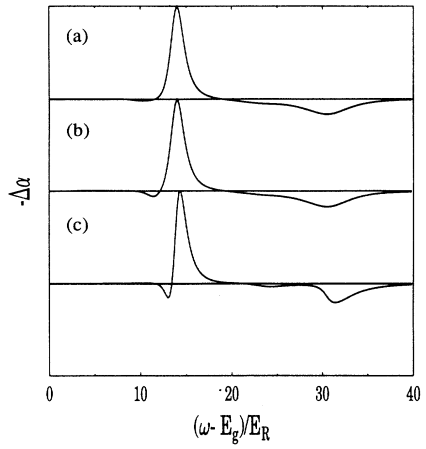

FIG. 3. Theoretically calculated differential absorption, $-\Delta\alpha L$, for different distributions of quantum-dot sizes. The distribution function is step Gaussian with a varying step position to simulate the effects of the saturator beam (see the text). Notice the shift of the induced absorptions on both sides of the bleaching and enhancement of the induced absorption below the bleaching.

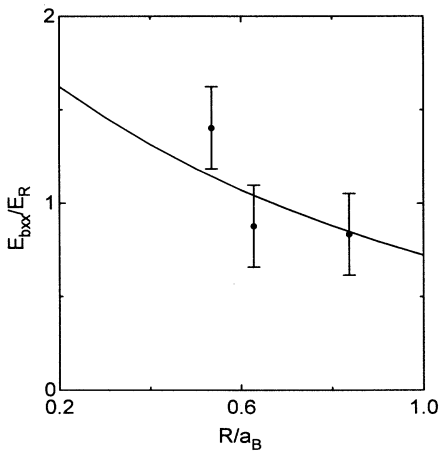

FIG. 4. Experimentally obtained biexciton binding energy as a function of dot size (data points). The theoretically calculated variation of biexciton binding energy with dot size is shown by the full curve. (The parameters used for the calculation were $m_e/m_h=0.2$, $\epsilon_2/\epsilon_1=10$, where ϵ_2, ϵ_1 are the dielectric constants of the semiconductor and embedding glass, respectively.)

binding energy by approximately 55%.

Even with the overestimation of biexciton binding energy from the experiment, we can see the qualitative agreement between the experiment (dots) and the calculation (solid line) as shown in Fig. 4. These results show that the larger confinement effect in smaller dots leads to enhancement of the biexciton binding energy. The observation of enhanced biexciton ground-state binding energy is similar to that reported in other quantum confined systems such as quantum wells[8–10] and quantum wires.[11]

It should be noted that luminescence experiments conducted in CuCl and CuBr microcrystallites[12–14] also suggest the enhancement of the biexciton binding energy with confinement. However, these experiments were done only for relatively large quantum dots where the enhancement effects are not as pronounced as in our system.

In conclusion, modification of conventional pump-and-probe spectroscopy by the use of an additional saturating laser beam reveals the ground state of the biexciton in quantum dots. This technique along with the narrow hole burning possible in our sample allowed an estimation of the biexciton binding energy. We observe enhancement of the biexciton binding energy with quantum confinement, confirming the theoretical predictions.

This work was supported by NSF, SDI/ONR, ARO, and JSOP. We would like to thank L. G. Mogilnaya for assistance in sample preparation and Dr. V. V. Golubkov for the small-angle x-ray-scattering analysis.

---

*Also at the Department of Physics, University of Arizona, Tucson, AZ 85721.

†Permanent address: Stepanov Institute of Physics, F. Skaryna Ave., 70 Minsk 220072, Belarus.

[1]Al. L. Efros and A. L. Efros, Fiz. Tekh. Poluprovodn. **16**, 1209 (1982) [Sov. Phys. Semicond. **16**, 772 (1982)].

[2]A. I. Ekimov and A. A. Onushchenko, Pis'ma Zh. Eksp. Teor. Fiz. **40**, 337 (1984) [JETP Lett. **40**, 1136 (1984)].

[3]L. E. Brus. J. Chem. Phys. **80**, 4473 (1984).

[4]Y. Z. Hu, S. W. Koch, M. Lindberg, N. Peyghambarian, R. Pollock, and F. F. Abraham, Phys. Rev. Lett. **64**, 1805 (1990).

[5]K. I. Kang, B. P. McGinnis, Sandalphon, Y. Z. Hu, S. W. Koch, N. Peyghambarian, A. Mysyrowicz, L. C. Liu, and S. H. Risbud, Phys. Rev. B **45**, 3465 (1992).

[6]U. Woggon, S. Gaponenko, W. Langbein, A. Uhrig, and C. Klingshirn, Phys. Rev. B **47**, 3684 (1993).

[7]Y. Z. Hu, M. Lindberg, and S. W. Koch, Phys. Rev. B **42**, 1713 (1990).

[8]R. C. Miller, D. A. Kleinmann, A. C. Gossard, and O. Munteanu, Phys. Rev. B **25**, 6545 (1982).

[9]D. A. Kleinmann, Phys. Rev. B **28**, 871 (1983).

[10]Q. Fu, D. Lee, A. Mysyrowicz, A. V. Nurmikko, R. L. Gunshor, and L. A. Kolodziejski, Phys. Rev. B **37**, 8791 (1988).

[11]L. Banyai, I. Galbraith, C. Ell, and H. Haug, Phys. Rev. B **36**, 6099 (1987).

[12]R. Revy, L. Mager, P. Gilliot, and B. Hönerlage, Phys. Rev. B **44**, 11 286 (1991).

[13]T. Itoh, F. Jin, Y. Iwabuchi, and T. Ikehara, in *Nonlinear Optics of Organics and Semiconductors,* edited by T. Kobayashi (Springer, Berlin, 1989), p. 76.

[14]U. Woggon, O. Wind, W. Langbein, O. Gogolin, and C. Klingshirn (unpublished).